Samander Ali Malik[1,2,*], Recep Türkay Kocaman[1], Thomas Gereke[1], Dilbar Aibibu[1], Chokri Cherif[1]

Prediction of the Porosity of Barrier Woven Fabrics with Respect to Material, Construction and Processing Parameters and Its Relation with Air Permeability

DOI: 10.5604/01.3001.0011.7306

[1] Technische Universität Dresden, Institute of Textile Machinery and High Performance Material Technology, 01062 Dresden, Germany
* E-mail: samander_ali.malik@tu-dresden.de

[2] Mehran University of Engineering & Technology, Department of Textile Engineering, 76062 Jamshoro, Sindh, Pakistan
* E-mail: samander.malik@faculty.muet.edu.pk

Abstract
Porosity is one of the most important characteristics of fabrics that dictate the permeability and retention properties of fabrics. Several technical uses require textiles with a combination of definite permeability and retention properties. Besides filtration, surgical textiles require these contrary properties to offer an effective barrier against particle laden fluids, such as bacteria and viruses, together with added wearer comfort. Pore size and pore size distribution are important characteristics to determine the permeability and retention behaviour of multifilament barrier textiles by influencing the effective porosity, which can be tailored according to end use requirements by material, weave construction and processing factors. The present research was aimed at developing the relationship that material, construction and loom parameters have with porosity in terms of the mean pore size and mean flow pore size of the fabric, and thereby with air permeability. To map such nonlinear complex relations, an artificial neural network (ANN) was employed. From the findings, it was observed that the porosity of barrier fabrics can be predicted with excellent accuracy using an ANN.

Key words: *barrier fabrics, porosity, permeability, prediction, artificial neural network.*

Introduction

High density multifilament woven fabrics are used for several technical applications which require definite permeability and retention properties in combination. In addition to use in filter technology, the utilisation of textile structures, especially in the case of protective clothing (surgical protective textiles, protective clothing against chemicals, clean room clothing for the semiconductor and pharmaceutical industries), has to meet contradictory requirements with regard to barrier properties (water permeability, particle retention) and comfort properties (air and water vapour permeability). Porosity (and consequently permeability) is also of very vital importance from the composite manufacturing impregnation point of view, such as resin infusion moulding. Sieminski and Hotte [1] described porosity as the fraction of the total volume of void spaces to the total volume, and when the voids become accessible to fluid to pass through, this results in permeability. The relationship between the permeability and porosity of normal density fabrics, where the fluid mainly flows through inter-yarn interstices, is well established. Several researchers [2-6] have developed theoretical and analytical air permeability models using the different porosity features of fabric. In the case of highly dense multifilament fabrics, where the pores cannot be observed by the naked eye, the flow mechanism is governed by both the inter-yarn and intra-yarn pore morphology, such as the number, size, shape, texture and arrangement of pores.

Pore size and pore size distribution are important characteristics to estimate the permeability and retention behaviour of multifilament barrier textiles by influencing the effective porosity (the portion of the total porosity which permits fluid to pass through) of the fabric, which largely depends upon the inter-yarn and intra-yarn pores [7]. Even at smaller fabric porosities of approx. 6%, the inter-yarn pores contribute 89-99% of the permeability [8]. This emphasises that inter-yarn voids (mesopores) play a very important role in estimating the permeation and retention tendencies of multifilament woven fabrics. Other factors also have an influence, but due to their structural complexities they are difficult to measure. Fabric porosity and permeability can be tailored in accordance with intended end use requirements by various material, weave construction and processing factors [9-11]. These factors seldom act individually, rather their underlying interactions affect the performance of barrier fabrics.

In this context, it is vital to develop a model which correlates the pore sizes of barrier fabrics with their constructional, material dependent and processing factors. Most textile processes are nonlinear and dynamic in nature. Therefore, to solve such complex nonlinear problems, the artificial neural network (ANN) is proven to be an effective tool. Since its beginnings in the late twentieth century, it has been widely used for textile machine optimisation [12], yarn and fabric property prediction, including antibacterial and hydrophobicity [13-15], and pattern recognition [16] problems. Moreover it has also been used successfully to predict the pore size of nonwoven and ultrafiltration membranes [17, 18]. Processing factors such as the metering pump frequency, die to collector distance and mesh belt frequency of melt blown non-woven fabrics were formerly used to train the network, whereas the solute separation and solute diameter were later employed to train the ANN. Besides that, it is also employed to predict the air permeability of dense woven fabrics [19]. It is evident from the literature cited herein that there is dearth of published research on the prediction of the pore size of multifilament barrier fabrics using material, fabric construction and processing factors.

The pore size and pore distribution of fabrics, filters and membranes can be measured with several methods such as mercury intrusion porosimetry [7, 20], bubble point [21], capillary flow porometry [22, 23], image analysis techniques [11, 24, 25], and the liquid displacement method [26, 27]. By using standard measuring equipment, the liquid displacement method provides important information

Table 1. *Impact of textile technological factors on pore size.*

Source of influence	Degree of influence on pore size	
	Micro pores	Meso pores
Multifilament yarn fineness	+	+++
Filament cross-section	+++	+
Filament fineness	+++	+
Yarn density	++	+++
Weave type	+	+++
+++ very important, ++ important, + not very important		

Table 2. *Yarn specifications.* ***Note:*** ** diameter was measured according to* ***Equation (1)****.*

Yarn specifications		Yarn 1	Yarn 2	Yarn 3	Yarn 4
		TREVIRA Multifilament 100 dtex f40 flat	TREVIRA Multifilament 100 dtex f128 flat	TREVIRA Multifilament 100 dtex f80 textured	TREVIRA Multifilament 150 dtex f48 flat
Yarn diameter, mm*		0.096	0.096	0.096	0.117
Filament fineness, dtex		2.5	0.8	1.25	3.125
Filament diameter, µm*		15	8.6	10.7	16.9
Use	Warp yarn	x			
	Weft yarn	x	x	x	x

regarding material porosity. As discussed earlier, theoretical models based on pore size data result in higher prediction errors because of the experimental inaccuracies in the measurement of pore size. The porosimeter PSM 165 (Topas GmbH, Germany), which has excellent measuring precision, measures the pore size of barrier woven fabrics, filters, membranes and non-woven fabrics in terms of the weighted mean pore size of the complete pore size distribution of a particular sample. The value of the weighted mean pore size is more realistic because it covers all type of pores according to their weighted permeability from the pore size distribution. Therefore, in current research, the weighted mean pore size (MPS), mean flow pore size (MFPS) and pore size distribution are measured using the liquid displacement method to train the neural network.

Material and methods

Materials

Polyester (PES) is a commonly used synthetic fibre to produce barrier fabrics, because of its wide variety of available fibre fineness, texture, cross-section and added functionalities, coupled with excellent physical properties. With the use of micro-fibres, it extends excellent drapability and softness. Due to these advantageous properties, it enables the manufacturer to develop woven barrier fabrics with defined densities and tailored pore morphology [9, 10]. Aibibu [10] categorized the effect of technological parameters on pore morphology, as stated in ***Table 1***.

A data set of 52 fabrics was generated comprising 28 and 24 patterns of plain (P 1/1) and twill 2/2Z (T 2/2Z) weave, respectively, following two trial matrices. The first was used to record the effect of loom dynamics and the second was designed to record the effect of weft density, yarn and filament fineness and texture on the pore sizes of dense multifilament woven fabrics. The specifications of yarns used in the current research are stated in ***Table 2***. The theoretical diameter of yarns and filaments was calculated as follows:

$$D\,[mm] = \left(\sqrt{\frac{T_y \times 4}{\pi \times \rho_y \times 10^5}}\right) \times 10 \quad (1)$$

where D is the diameter of the yarn/filament, T_y the fineness in tex; and ρ_y the material density in g/cm^3 (PES = 1.39 g/cm^3).

Fabric and loom parameters

The pore size and pore size distribution of dense multifilament woven fabrics are highly influenced by the weave type, weave density, yarn fineness and filament fineness, whereas the effect of processing parameters is limited [9]. For the sake of higher loom efficiencies, better process handling and cost effectiveness, higher warp densities and optimum weft densities are advisable, which is more important for dense fabrics, where weaving is more challenging, Therefore the warp density was set at 68 ends/cm, while the weft density was varied between 22-36 picks/cm for P 1/1 and 39-48 picks/cm for the T 2/2Z weave. The size of inter-yarn pores is usually measured from the geometrical parameters of the fabric unit cell, which in turn depends upon the yarn fineness (yarn diameter) and weave design; whereas intra-yarn pores are influenced by filament fineness, as indicated in ***Table 1***. To avoid too many input variables to train the ANN, in the current research the weave density index (WDI) is calculated according to Walz-Luibrand [28] using the densities measured. It is a unified input in which the warp and weft density, warp and weft yarn diameter and count, and material density are merged together, reducing the complexity of the model by decreasing the number of inputs. Fabric density is theoretically calculated as follows:

$$WDI = c \cdot (D_{wp} + D_{wf})^2 \cdot \frac{(N_{wp} \cdot N_{wf})}{100} \quad (2)$$

where c is the weave coefficient (plain 1/1 = 1, twill 2/2 = 0.56), D the yarn diameter in mm (calculated according to ***Equation (1)***), and N is the number of yarns per cm. Subscripts *wp* and *wf* represent warp and weft yarns, respectively.

The weaving of PES multifilament woven barrier fabrics was carried out on a Dornier PTS4/S EasyLeno® double rapier weaving machine (Lindauer Dornier GmbH, Germany) with a conventional shedding mechanism. Asymmetric shed geometries (lower shed > upper shed) were selected for all fabrics, and to prevent width contraction, a full-width temple guide was employed. Weaving was performed according to a trial matrix (***Table 3***), which comprises two sub-trial plans. Trial plan a (samples 1-32) served to assess the effect of machine processing parameters, such as the machine speed (rpm) and shed closing time (°) on the pore size of fabrics, whereas trial plan b (samples 33-52) was used to record the influence of yarn and fabric parameters, as given in ***Table 3***. Loom dynamics also influence the yarn tension forces, which affect the crimp interchange and yarn flattening on crossovers, thereby impacting the pore morphology of the fabric (9,29). To record the influence of processing factors, the loom speed was varied between 200 and 450 rpm. Beyond this range weaving was not possible with higher thread densities, whereas the warp sheet closing time (angle °) was varied between -10° and +15° from the default 330° (i.e. 320°-345°). After weaving, the fabrics were desized, washed and thermally fixed.

Measurement of pore size and pore size distribution

Liquid displacement porosimetry using a pore size meter – PSM 165 (Topas GmbH, Germany) was performed following the standards ASTM E1294-89 and ASTM F316-03 with a capillary constant of 28.6. Topor (a perfluorocarbon of surface tension 16 mN/m) was used as the test liquid. Measurements were carried out using a standard measuring head of 2.01 cm², and the flow rate range and maximum pressure were set at 0.06-70 l/min and 2000 mbar, respectively. PSM 165 is an automated instrument which provides not only the pore size distribution range between 0.15 µm and 250 µm but also delivers the weighted mean, median and model pore sizes, the mean flow pore size (pore size diameter corresponding to the pressure drop, where the wet flow value is half of the dry flow) and the bubble point.

Air permeability measurements

Test specimens were acclimatised under standard atmospheric conditions for textiles for 24 hours according to DIN EN ISO 139: 2005+A1:2011. The through thickness air permeability *(K)* of the fabric was measured in accordance with standard test method DIN EN ISO 9237:1995 using an FX 3300 (Textest AG, Switzerland) air permeability tester. The measurements were performed using a 20 cm² test head and the pressure drop was set to 200 Pa. Five measurements were taken from each right and left side and centre of the fabric to complete a total of 15 measurements across the width of a 1 m² fabric sample. The mean value of fifteen measurements was used for analysis. To exclude any impact of air leakage between the fabric and sample holder, the measurements were repeated with a plastic sheet and the value of permeability *(K2)* recorded was subtracted from the permeability value measured with the fabric only *(K1)*.

$$K = K_1 - K_2 \qquad (3)$$

Artificial neural network

Since its beginnings in the late 20th century, when Rumelhart, Hinton and Williams [30] presented a backpropagation algorithm to train multilayer perceptron (MLP) by overcoming the limitations of early perceptron type networks, as identified by Minsky and Papert in 1969 [31], the artificial neural network (ANN), or simply neural network, is a widely accepted soft computing technique to solve

Table 3. *Trial matrix for manufacturing of model weaves.* ***Note:*** *superscripts * and + represent set and measured weft densities, whereas ++ is for the Wlaz-Luibrand Index.*

Model weave	Weave	Weft, cm^{-1}	Weave density^{++}	Weft Yarn	Loom speed, rpm	Shed closing, °	Mean pore size, µm	Air permeability
M1	P 1/1	36*/40^{+}	1.07	Yarn 1	450	330	2.25	9.05
M2	P 1/1				200		2.39	9.9
M3	P 1/1				300		2.8	10.49
M4	P 1/1				400		2.55	8.37
M5	T 2/2Z	48*/50^{+}	0.8		450		5.31	31.1
M6	T 2/2Z				200		4.98	27.1
M7	T 2/2Z				300		5.13	29.89
M8	T 2/2Z				400		5.47	26.66
M9	P 1/1	36*/40^{+}	1.07		450	320	2.72	9.24
M10	P 1/1				200		2.67	9.47
M11	P 1/1				300		2.46	8.52
M12	P 1/1				400		2.78	8.59
M13	T 2/2Z	48*/50^{+}	0.8		450		5.03	32.37
M14	T 2/2Z				200		5.92	27.05
M15	T 2/2Z				300		6.3	29.58
M16	T 2/2Z				400		6.12	28.41
M17	P 1/1	36*/40^{+}	1.07		450	335	2.44	9.38
M18	P 1/1				200		2.51	8.8
M19	P 1/1				300		2.48	8.84
M20	P 1/1				400		2.57	8.58
M21	T 2/2 Z	48*/50^{+}	0.8		450		5.44	31.01
M22	T 2/2 Z				200		4.8	28.97
M23	T 2/2 Z				300		5.25	29.71
M24	T 2/2 Z				400		5.1	27.72
M25	P 1/1	36*/40^{+}	1.07		450	345	2.59	8.93
M26	P 1/1				200		2.46	8.2
M27	P 1/1				300		2.62	8.45
M28	P 1/1				400		2.7	10.25
M29	T 2/2Z	48*/50^{+}	0.8		450		5.24	31.81
M30	T 2/2Z				200		4.87	30.23
M31	T 2/2Z				300		5.68	33.23
M32	T 2/2Z				400		4.79	29.33
M33	P 1/1	22*/24^{+}	0.64	Yarn 1	300	330	3.91	38.47
M34	P 1/1	27*/29^{+}	0.78				3.57	32.91
M35	P 1/1	36*/40^{+}	1.07				2.8	10.49
M36	T 2/2Z	39*/41^{+}	0.66				5.7	37.14
M37	T 2/2Z	48*/50^{+}	0.80				5.13	29.89
M38	P 1/1	22*/24^{+}	0.64	Yarn 2			3.76	23.75
M39	P 1/1	27*/29^{+}	0.78				3.31	13.07
M40	P 1/1	36*/40^{+}	1.07				2.68	7.87
M41	T 2/2Z	39*/41^{+}	0.66				5.42	28.28
M42	T 2/2Z	48*/50^{+}	0.80				4.68	17.01
M43	P 1/1	22*/24^{+}	0.64	Yarn 3			3.73	30.47
M44	P 1/1	27*/29^{+}	0.78				3.07	17.83
M45	P 1/1	36*/40^{+}	1.07				2.1	7.12
M46	T 2/2Z	39*/41^{+}	0.66				5.17	30.45
M47	T 2/2Z	48*/50^{+}	0.80				4.21	23.11
M48	P 1/1	18*/19^{+}	0.63	Yarn 4			5.68	80.19
M49	P 1/1	22*/24^{+}	0.79				4.63	40.63
M50	P 1/1	29*/32^{+}	1.07				3.02	17.69
M51	T 2/2Z	31*/34^{+}	0.67				11.31	87.23
M52	T 2/2Z	39*/42^{+}	0.80				9.52	70.23
Warp density measured: P 1/1 = 73 ends/cm and T 2/2Z = 78 ends/cm								

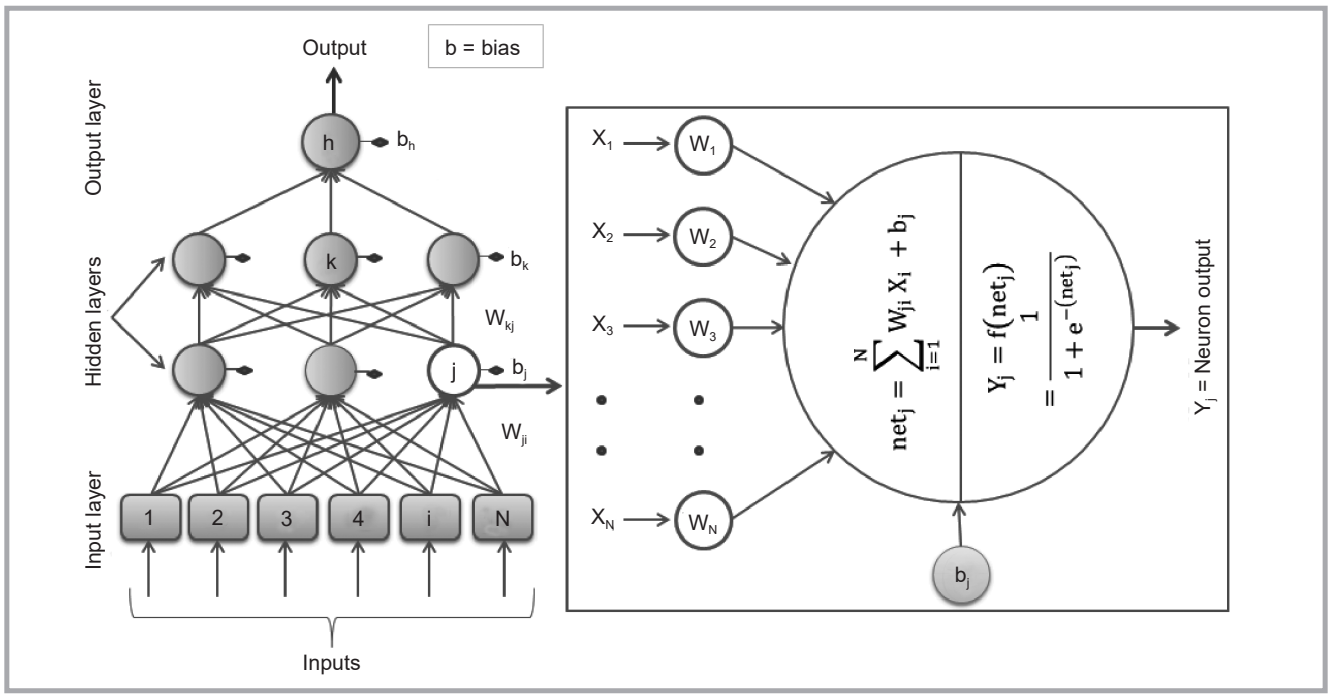

Figure 1. *Schematic diagram of artificial neural network.*

process optimisation, prediction and pattern recognition problems in a wide range of science and engineering disciplines. ANNs are adoptive systems inspired by the human nerve cell system; hence, like the human brain, they also learn and develop rules by experience. An ANN gets information from the environment through a training and learning process, and the knowledge learnt is stored in synaptic weights.

Feedforward multilayer perceptron (MLP) is a commonly used algorithm. From functionality point of view, MLP's architecture is divided into three parts: input, hidden and output neurons. The input neurons get training inputs to the network through interfacing with the outside world. The mathematical operations and functions are performed by hidden/intermediate neurons, whereas the network's predicted outputs are delivered by the output neuron(s). The neurons in the preceding layer are connected to the succeeding layer by connection weights to mimic the ability of the human brain.

Multilayer networks are commonly trained by using a backpropagation algorithm. Iterative training is performed in three steps: firstly the inputs are presented to the network along its feedforward path, and mathematical functions are performed. In the next step, the network predictions are compared with set targets, and the error signal is computed.

In the last step, if the network does not meet the user's specified stopping conditions, the algorithm first calculates the new weight and then updates the weight and bias variables for the new iteration.

The architecture of a multilayer ANN and operations performed by a nonlinear neuron are schematically illustrated in ***Figure 1***. Training begins with the presentation of inputs X_i through the i^{th} neuron of the input layer to the j^{th} neuron (succeeding layer) by weight factor W_{ji}. The weighted inputs are summed up, the bias weight added, and then the network input function net_j converts the presented i^{th} layer inputs into a new value as follows:

$$\mathrm{Net_j} = \sum_{i=1}^{N} X_i W_{ji} + b_j \qquad (4)$$

Backpropagation requires a differentiable transfer function; therefore in the present model (as illustrated in ***Figure 1***, right side) a logsigmoid is used as the transfer function in hidden layer neurons. The summed weighted inputs, net_j, are fed to the transfer function, and transformed into the neuron output Y_j (output of the current layer becomes the input of the following layer neurons) as below:

$$Y_j = f(\mathrm{net_j}) = \frac{1}{1 + e^{-(\mathrm{net_j})}} \qquad (5)$$

At the end of each iteration, the network predicted outputs (O_i) are compared with the target outputs (T_i) and the error signal is computed in terms of the mean squared error MSE, which is calculated as

$$\mathrm{MSE} = \frac{1}{N}\sum_{i=1}^{N}(T_i - O_i)^2 \qquad (6)$$

where N is the number of patterns.

For the current research, the Matlab® neural network toolbox function 'trainbr' was used, which is an incorporation of the Levenberg-Marquardt (LM) optimisation technique and automated Bayesian regularisation into back propagation. The Back propagation computes the Jacobian matrix of the error function with respect to weights and biases, and variables are modified by LM optimisation

$$\Delta W = (J^T J + \mu I)^{-1} J^T e \qquad (7)$$

where, J represents the Jacobian matrix of first derivatives of the error with respect to weights and biases; I is the identity unit matrix, e the error vector, T the matrix transposition, and μ is the learning parameter. Interested readers are referred

Table 4. *Network architecture and parameters.*

Model parameters	
Network architectures	6-[3-3]$_2$-1
Learning rate, σ	0.2
Constant μ	0.3
Performance goal	0.0001
Max. epochs	2000

to literature [32-35] for details about the LM method and Bayesian regularisation.

The number of layers and neurons were selected using the hit and trial process by training several networks with different architecture and parameters. Moreover the logistic sigmoid (logsig) and linear (purelin) transfer functions were selected for hidden and output neurons, respectively, and the mean squared error (MSE, ***Equation (6)***) was used as the performance function. However, the network performance is reported in terms of the mean absolute error (MAE) and root mean square deviation (RMSD), calculated as follows:

$$MAE = \frac{1}{N}\sum_{i=1}^{N}|T_i - O_i| \quad (8)$$

$$RMSD = \sqrt{\frac{1}{N}\sum_{i=1}^{N}(T_i - O_i)^2} \quad (9)$$

Before training, the whole data set was normalised between 0 and 1 and subsequently divided randomly into training and testing sub sets; 42 data patterns were selected for network training and the remaining 10 patterns used to evaluate the network performance for unseen data.

By varying the network architecture and parameters, several networks were trained to minimise the error and obtain a model with better generalised capabilities. On the basis of the hit and trial of a two hidden layer network, three neurons in each layer were selected. The architecture and training parameters of the model selected are given in ***Figure 1*** and ***Table 4***.

Results and discussion

The neural network was trained using the weave type, weave density, filament fineness, filament type, loom speed and shed closing time, the input levels of which are given in ***Table 6***. The training and testing performances of the ANN models developed for the weighted mean pore size (MPS) and mean flow pore size (MFPS) are illustrated in ***Figure 2***. It can be observed from the following figure that the neural network learnt the underlying interaction between training inputs and output variables well. Apart from some minor deviations in a few samples, the network predictions match well with experimental scores. The training performance of both models is almost identical,

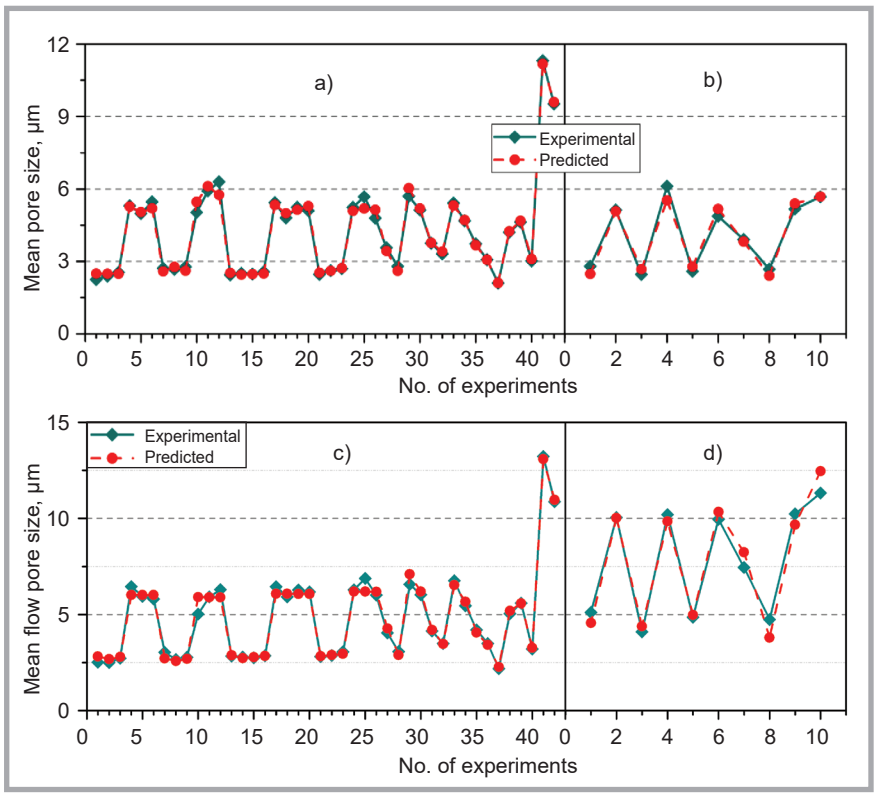

Figure 2. *Performance of model developed: ANN-MPS – a) training, b) testing; ANN-MFPS – c) training, d) testing.*

but the testing performance of ANN-MPS is slightly better than for ANN-MFPS.

The training error of both models is within 2%, whereas the testing error is within 3%. The MAE and RMSD values of ANN-MPS are 0.23 and 0.28 µm, respectively, on a scale of 2.1-11.31 µm. Moreover MAE and RMSD values for ANN-MFPS are recorded as 0.31 and 0.68 µm, respectively, on a scale of 2.19-13.22 µm, as stated in ***Table 5***. This excellent performance for unseen data indicates that the ANN has generalised well without any evident overfitting.

Regression analysis is another important measure to check ANN performance. ***Figures 3.a, 3.b*** reflects the excellent relationship between the experimental and predicted mean pore size of barrier fabrics. R^2 values of the linear fitted model between predicted and experimental scores for training and testing are 0.990

Table 5. *Performance of model selected.*

Performance parameters	ANN-MPS		ANN-MFPS	
	Training	Testing	Training	Testing
MAE, %	1.44	2.45	1.61	2.81
MAE, µm	0.13	0.23	0.18	0.31
RMSD, µm	0.18	0.28	0.25	0.68
Max. error, %	0.54	0.59	-0.88	-0.99
Min. error, %	0.00	-0.01	0.001	0.01

Table 6. *Input levels and middle values for trend analysis.*

Inputs	Input levels	Middle values
Weave float	P 1/1, T 2/2Z	1 for plain weave 2 for twill weave
Weave density (Walz-Luibrand Index)	P 1/1 – 0.64, 0.8, 1.07 & T 2/2Z – 0.64, 0.8	0.8
Weft filament fineness, dtex	0.78, 1.25, 2.5, 3.125	2.5
Weft yarn type	Flat (0), textured (1)	Flat
Loom speed, rpm	200, 300, 400, 450	300
Shed closing time, °	320, 330, 335, 345	330

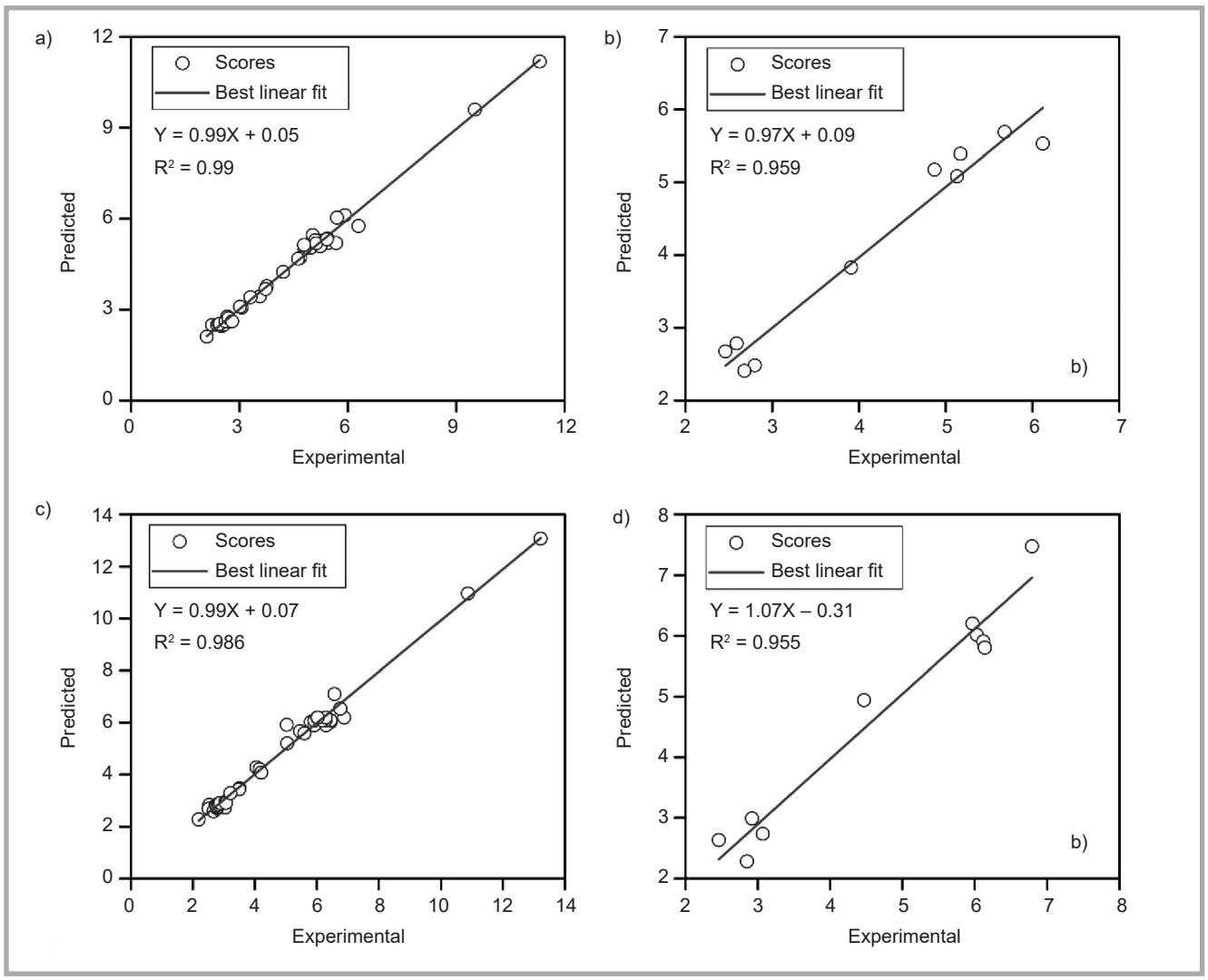

Figure 3. *Regression analysis experimental vs. predicted values (in µm): ANN-MPS – a) training, b) testing; ANN-MFPS – c) training, d) testing.*

and 0.959, respectively, which means that more than 96% variance in the dependent variable is explained by the independent variables. This is also obvious from the slope and intercept of the linear models as well. Almost similar model regression analysis results can be observed for ANN-MFPS in ***Figure 3.c, 3.d***.

These findings advocate that it is plausible to predict the mean pore size and mean flow pore size of PES multifilament barrier fabrics using material, fabric construction and processing parameters with excellent accuracy using an artificial neural network. It also confirms the prediction power and accuracy of an artificial neural network.

Trend analysis of model developed

Trend analysis is a method to check the influence of individual input variables on the model output. In this technique one input is varied at a time to its factor levels, whereas the other input variables are kept to their middle value, with the change in output being recorded at each level. This process is repeated for all variables. The input levels and middle values are given in ***Table 6***.

Results of the trend analysis for ANN-MPS are illustrated in ***Figure 4.a-4.f***. It is evident from (a) that the pore size of plain woven fabric is lower than for twill weave using the same weave index, which is in agreement with experimental results. As the permeability of fabric is directly influenced by its porosity, a similar trend is observed in the experimental air permeability values stated in ***Table 3***. Weave type mainly impacts the inter-yarn pores. Higher float length weaves (satin/twill) have bigger inter-yarn pores as compared to small float length constructions like plain weave.

The mean pore size of barrier fabrics is decreased by increasing the weave density, as shown in ***Figure 4.b.*** A similar trend is also observed with the weft filament fineness: the finer the filament (similar yarn fineness), the lower the mean pore size (***Figure 4.c***). The change is minor – from 0.78 to 1.25 dtex filament; thereafter a substantial increase in MPS is observed as the filament fineness decreased to 3.125 dtex, due to finer filaments increasing the yarn packing and reducing inter-filament gaps. Likewise fabric woven with textured weft yarn has somehow a lesser mean pore size than those woven with flat weft yarns (***Figure 4.d***).

The influence of the loom speed and shed closing time is depicted in ***Figure 4.e, 4.f***, which reflects that the mean pore size slightly increases with increasing loom speed. However, with respect to the shed closing time, the effect is random and lacks a certain trend. In plain weave a slight increase in the mean pore size is

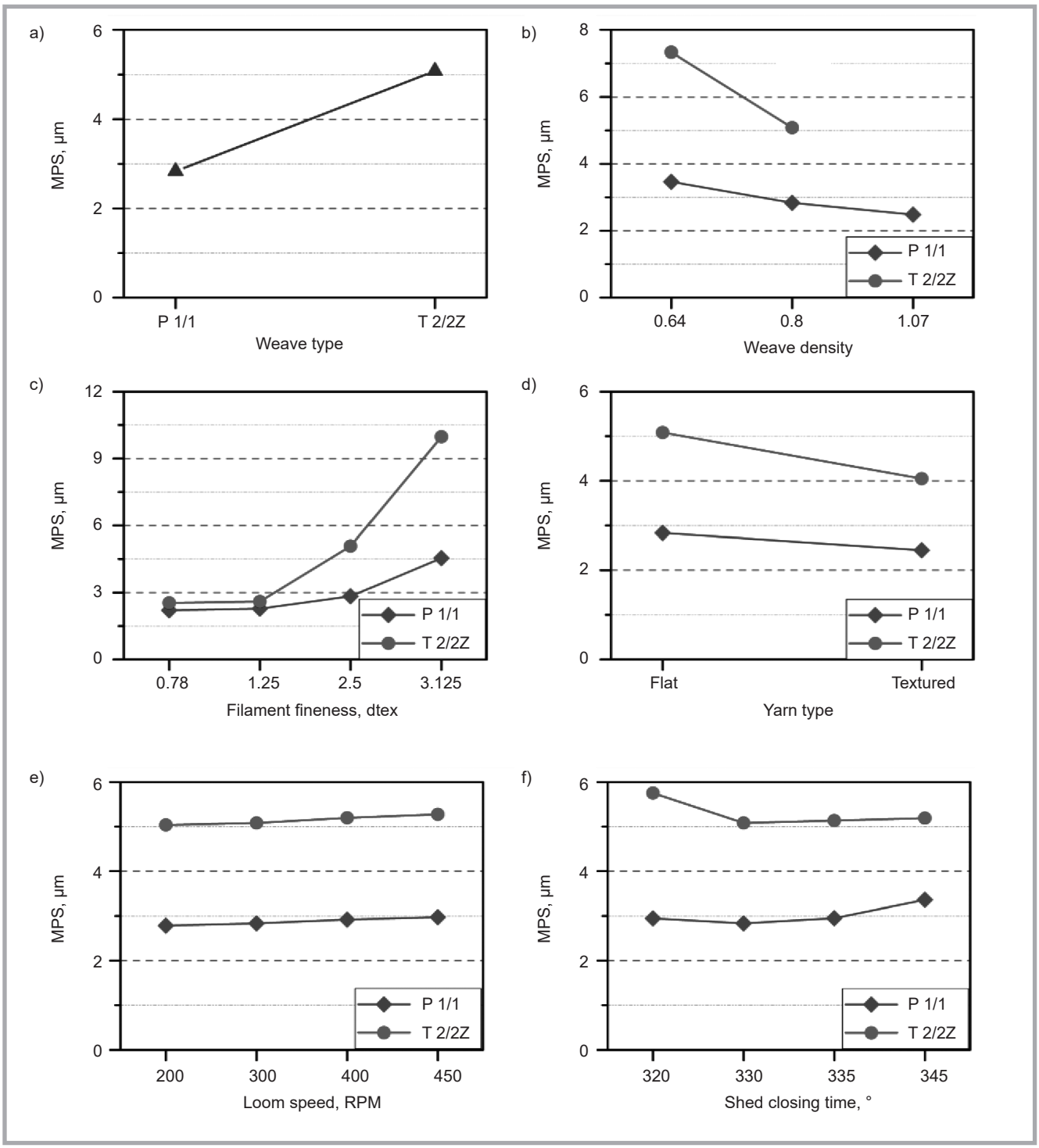

Figure 4. *Trend analysis using ANN model developed: effect of (a) weave type, (b) weave density, (c) weft filament fineness, (d) yarn texture, (e) loom speed and (f) shed closing time of mean pore size of barrier woven fabrics.*

observed with respect to the shed closing time, whereas for twill fabric woven at 320° the shed closing time shows a higher MPS; thereafter it is almost constant.

The findings of the trend analysis are in agreement with the experimental results, which suggest that the model developed has simulated the input-output relationship well. Thus this model can be used for practical problem within its learnt domain to predict the mean pore size of barrier woven fabrics.

Moreover, by using the yarn crimp measured from the fabric model and information from the porosity ANN model developed in the present research, new weave geometries can be realised using microscale simulation with the finite element method for virtual simulation. Geometric models based on selected parameters such as yarn crimp, yarn and filament fineness, weave type and weave density can be used to predict the porosity, permeability and other structural properties of dense fabrics in relaxed and under loading situations using any the fluid dynamics procedure. However, for confirmation of the geometric models, the porosity measured can be validated with the neural network developed model as well as by available experimental data. For this purpose a microscale

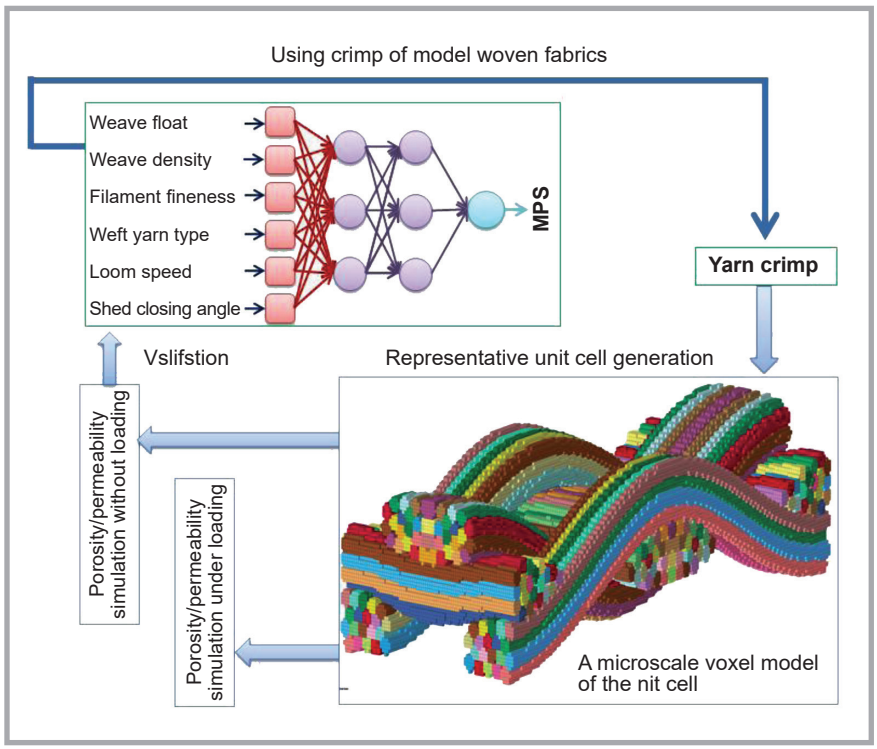

Figure 5. *Geometrical model for simulation of porosity/permeability in relaxed and loaded situations.*

voxel model of a plain weave's unit cell is being developed and simulations will be performed later. The concept is pictorially explained in ***Figure 5***. The voxel model can be obtained from a finite element model of the fabric that is built according to the method described in [36], which uses the input of geometrical parameters such as warp and weft densities and yarn crimp from the ANN model. The finite elements are then transferred into volumetric voxels in order to obtain the porosity of the fabric more efficiently, because voxel geometry is the native input format used by several software modules like FlowDict and FilterDict.

Relationship between mean pore size and air permeability

The coefficient of correlation is a measure of the strength and direction of the linear relation between two variables. It is established that the permeability of materials depends upon their porosity. In woven fabrics porosity is described as the number, size, shape, texture and arrangement of inter-yarn and intra-yarn pores [6]. Pore size is one of the important factors which comprise the greatest part of porosity, and consequently permeability; other factors also have an influence, but they are difficult to measure.

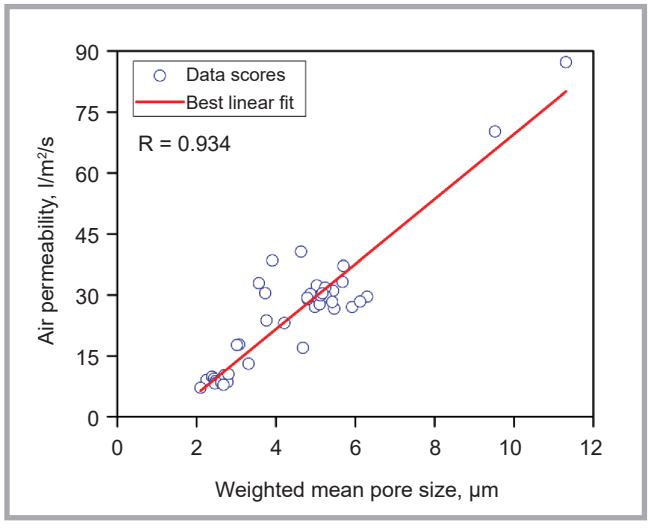

Figure 6. *Correlation between mean pore size and air permeability of barrier woven fabrics.*

The linear fitted regression model given in ***Figure 6*** demonstrates a very strong positive correlation between the MPS [µm] and air permeability [l/m²/s] of the barrier fabric with the coefficient of correlation, an R value of 0.934 ($R^2 = 0.87$).

$$Air\ permeability = 8 \times MPS - 10.4 \quad (10)$$

It reflects that as the MPS of the fabric increases, the air permeability also increases, and vice versa, which is also obvious from the regression equation. It confirms the theoretical knowledge that air permeability mainly depends upon inter-yarn pores. Furthermore the outcomes also validate the accuracy of the measuring technique used for MPS measurement. Therefore the use of the artificial neural network models in the above-mentioned research is advised, which could save experimental time and cost. Furthermore an ANN could be beneficial in the manufacturing of hybrid composites for tailored mechanical properties.

From the findings above, it is inferred that MPS can be predicted from material, fabric and processing parameters using an ANN, and the results can also be used to determine air permeability.

Conslusions

Porosity in terms of the mean pore size (MPS) and mean flow pore size (MFPS) of PES multifilament barrier woven fabrics was successfully predicted with excellent accuracy using artificial neural networks. ANN-MPS and ANN-MFPS were trained separately using similar input variables. From the test performance it can be inferred that both models have learnt the underlying interactions between input and output variables. The MAE and RMSD of ANN-MPS observed are 0.23 and 0.28 µm, with an R^2 value of 0.959, which means that 96% variance in the dependent variable is explained by independent variables. Likewise the test error in terms of the MAE and RMSD of ANN-MFPS were recorded as 0.31 and 0.68 µm, respectively, with a coefficient of determination of 0.955.

The model developed for the mean pore size was further evaluated through trend analysis. It was observed that porosity is significantly influenced by the weave type, weave density, and filament fineness, and is moderately effected by the yarn texture. A slight change in loom pa-

rameters was also noted. Furthermore it was observed that the air permeability of barrier fabrics can be determined using the weighted mean pore size calculated from the pore size distribution.

From these findings it is inferred that ANN is a powerful prediction tool to determine the MPS from material as well as fabric and processing parameters with excellent accuracy, and the prediction results can be used to determine air permeability as well. This will eliminate the trial and error procedure, which saves time and money.

Acknowledgements

The corresponding author, Samander Ali Malik, would like to acknowledge the financial support of the Graduate Academy of TU-Dresden for providing a short term "completion and wrap-up phase" grant. He would also like to express his sincere gratitude to the Higher Education Commission (HEC) Pakistan and German Academic Exchange Service (Deutscher Akademischer Austauschdienst, DAAD) for the granting of a PhD scholarship. We also acknowledge the German Research Foundation (DFG) for financing this research through project DFG CH 174/38-1.

Declaration of conflicting interests

The authors declare no potential conflict of interest with respect to the research, authorship, and/or publication of this article.

Funding

The author(s) disclose the financial support of Deutsche Forschungsgemeinschaft [DFG CH 174/38-1] for the research, authorship, and publication of this article.

References

1. Sieminski MA, Hotte G. The porosity of the textile materials. *Rayon Text Mon.* 1944; 25(12): 608-10.
2. Zupin Z, Hladnik A, Dimitrovski K. Prediction of one-layer woven fabrics air permeability using porosity parameters. *Text Res J.* 2012; 82(2): 117-28.
3. Ogulata RT, Mezarcioz S (Mavruz). Total porosity, theoretical analysis, and prediction of the air permeability of woven fabrics. *J Text Inst.* 2012;103(6):654-61.
4. Xu G, Wang F. Prediction of the Permeability of Woven Fabrics. *J Ind Text.* 2005; 34(4): 243-54.
5. Xiao X, Zeng X, Long a., Lin H, Clifford M, Saldaeva E. An analytical model for through-thickness permeability of woven fabric. *Text Res J.* 2012;82(5): 492-501.
6. Havlová M. Air Permeability and Constructional Parameters of Woven Fabrics. *FIBRES & TEXILES in Eastern Europe* 2013; 21 2(98): 84-89.
7. Burleigh EG, Wakeham H, Honold E, Skau EL. Pore-Size Distribution in Textiles. *Text Res J.* 1949; 19(9): 547-55.
8. Xiao X. *Modeling the Structure-Permeability Relationship for Woven Fabrics*. PhD Thesis, The Unievrsity of Nottingham, 2012.
9. Laourine E, Cherif C. Characterisation of barrier properties of woven fabrics for surgical protective textiles. *Autex Res J.* 2011; 11(2): 31-6.
10. Aibibu D. *Charakterisierung, Modellierung und Optimierung der Barriereeigenschaften von OP-Textilien*. PhD Thesis, Technische Universität Dresden, 2005.
11. Aibibu D, Lehmann B, Offermann P. Barrier effect of woven fabrics used for surgical gowns. *Autex Res J.* 2003; 3(4): 186-93.
12. Farooq A, Cherif C. Use of artificial neural networks for determining the leveling action point at the auto-leveling draw frame. *Text Res J.* 2008; 78(6): 502-9.
13. Malik SA, Arain RA, Khatri Z, Saleemi S, Cherif C. Neural network modeling and principal component analysis of antibacterial activity of chitosan/AgCl-TiO2 colloid treated cotton fabric. *Fibers Polym.* 2015; 16(5): 1142-9.
14. Malik SA, Farooq A, Gereke T, Cherif C. Prediction of blended yarn evenness and tensile properties by using artificial neural network and multiple linear regression. *Autex Res J.* 2016; 16(2): 43-50.
15. Malik SA, Saleemi S, Mengal N. Predicting hydrophobicity of silica sol-gel coated dyed cotton fabric by artificial neural network and regression. *Indian J Fibre Text Res.* 2016; 41(1): 67-72.
16. Behera BK, Mani MP. Characterization and Classification of Fabric Defects using Discrete Cosine Transformation and Artificial Neural Network. *Indian J Fiber Text Res.* 2007; 32(4): 421-6.
17. Jin G, Zhu C. Artificial Neural Network Modeling for Predicting Pore Size and Its Distribution for Melt Blown Nonwoven. *SEN'I GAKKAISHI*. 2015; 71(11): 317-22.
18. Ibrahim MZ, Norashikin MZ. Pore Size Prediction of Polyethersulfone Ultrafiltration Membranes Using Artificial Neural *Networks. J Nanosci Nanotechnol* 2010;10(9): 6211-5.
19. Malik SA, Kocaman RT, Kaynak HK, Gereke T, Aibibu D, Babaarslan O, et al. Analysis and prediction of air permeability of woven barrier fabrics with respect to material, fabric construction and process parameters. *Fibers Polym* [Internet]. 2017 Oct; 18(10): 2005-17. Available from: https://doi.org/10.1007/s12221-017-7241-5
20. Wakeham H, Spicer N. Pore-Size Distribution in Textiles-A Study of Windproof and Water-Resistant Cotton Fabrics*. *Text Res J.* 1949; 19(11): 703-10.
21. Bhatia SK, Smith JL. Application of the bubble point method to the characterization of the pore-size distribution of geotextiles. Geotech *Test J.* 1995; 18(1): 94-105.
22. Li D, Frey MW, Joo YL. Characterization of nanofibrous membranes with capillary flow porometry. *J Memb Sci.* 2006; 286(1-2): 104-14.
23. Kopitar D, Skenderi Z, Matijasic G. Influence of nonwoven fabric pore sizes on water vapor resistance. *Text Res J* [Internet]. 2017; Available from: http://journals.sagepub.com/doi/10.1177/0040517517700200
24. Angelova RA. Determination of the pore size of woven structures through image analysis. *Cent Eur J Eng.* 2012;2(1): 129-35.
25. Gong RH, Newton A. Image-analysis Techniques. Part I: The Measurement of Pore-size Distribution. J Text Inst [Internet]. 1992;83(2): 253-68. Available from: http://www.tandfonline.com/doi/abs/10.1080/00405009208631195
26. 316-03 AF. Standard Test Methods for Pore Size Characteristics of Membrane Filters by Bubble Point and Mean Flow Pore Test. ASTM International, West Conshohocken, PA. 2011. p. 1-7.
27. E1294-89(1999) A. Standard Test Method for Pore Size Characteristics of Membrane Filters Using. ASTM Int West Conshohocken, PA. 1999; 1-2.
28. Walz F, Luibrand J. Die Gewebedichte. *Text Prax.* 1947; 2:330-5.
29. Backer S. The Relationship Between the Structural Geometry of a Textile Fabric and Its Physical Properties Part IV: Interstice Geometry and Air Permeability. *Text Res J.* 1951; 21(10): 703-14.
30. Rumelhart DE, Hinton GE, Williams RJ. Learning representations by back-propagating errors. Nature. 1986; 323:533-6.
31. Minsky M, Papert S. Perceptrons. MIT Press, Cambridge MA; 1969.
32. Hagan MT, Menhaj MB. Training Feedforward Networks with the Marquardt Algorithm. *IEEE Trans Neural Networks*. 1994; 5(6): 989-93.
33. Marquardt DW. An Algorithm for Least Squares Estimation of Nonlinear Parameters. *J Soc Ind Appl Math.* 1963; 11(2): 431-41.
34. Wilamowski BM, Iplikci S, Kaynak O, Efe MO. An algorithm for fast convergence in training neural networks. In: *Proceedings IJCNN '01 International Joint Conference on Neural Networks* 2001, p. 1778-82.
35. MacKay DJC. Bayesian Interpolation. *Neural Comput*. 1992; 4(3): 415-47.
36. Döbrich O, Gereke T, Cherif C. Modeling of textile composite reinforcements on the micro-scale. *Autex Res J.* 2014; 14(1): 28-33.

Received 19.06.2017 Reviewed 11.12.2017